An approach to achieve all-angle, polarization-insensitive and broad-band self-collimation in 2D square-lattice photonic crystals

[1] Noori M., [1] Soroosh M. and [2] Baghban H.

[1] Faculty of Engineering, Shahid Chamran University of Ahvaz, Ahvaz, Iran, m-noori@phdstu.scu.ac.ir
[2] School of Engineering Emerging Technologies, University of Tabriz, Tabriz, Iran

Received: 24.12.2014

Abstract. We have investigated the possibility for achieving (in the same structure), an all-angle, polarization-insensitive and broad-band self-collimation (SC), one of the most urgent requirements in the field of optical integration. To obtain these attractive SC features in 2D square-array photonic crystals, we have used several strategies and performed testing calculations, using plane-wave expansion and finite-difference time-domain methods. We have not complicated the basic structure for the SC and ensured its simple geometry. The all-angle SC can arise when the optical material of a hole-type structure is high-index. Our results have testified that the SC in the hole-type structure is less dependent on the light polarization, if compared with a similar rod-type one. Our optimized SC structure has a bandwidth of $\Delta f/f_c = 2.61\%$ and supports the all-angle SC for both TE and TM polarizations at the expense of small (~ 3°) deviation of light from the unique collimation direction. Notice that the latter can be tolerated in many integrated optical devices.

Keywords: self-collimation, photonic crystals, equal-frequency contours, optical integrated circuits.

PACS: 42.82.-m, 42.82.Gw, 42.82.Et, 42.79.Gn
UDC: 621.3

1. Introduction

Self-collimation (SC) called also as self-guiding [1] or super-collimation [2] is one of the most attractive dispersion properties of photonic crystals (PCs), which has got a great attention of researchers. It refers to the optical conditions under which light propagates with no diffraction and divergence along a specific collimating direction. Earlier experimental and theoretical studies of the PCs have focused on photonic band gaps and several appropriate devices have already been developed [3]. But in the recent years, the studies have revealed that the photonic bands show unusual dispersion properties, which make them sources of several attractive effects [4, 5] such as negative refraction and left handedness [6–8], super-prism [9], slow light [10] and SC [2, 11–19] effects. Among these, the SC in PCs provides a brand new way of confining light propagation, which is different from conventional PC waveguides.

The SC effect has been initially demonstrated by Kosaka et al. [18] in 3D PCs and Wu et al. [17] in 2D PCs. Unlike spatial solitons, SC is a linear effect totally independent of light intensity, and involves no beam focusing or diffraction compensation due to optical nonlinearities. Instead, the PCs can be designed to have such dispersion properties that allow incident optical waves to be naturally collimated along certain directions [20]. The SC can benefit a large variety of applications related to wave guiding and light collection, e.g. waveguides for optical integrated circuits [21, 22], beam splitters [23, 24], optical switches [25], multiplexers [26], sensors [27], interferometers [28], wave plates [29], resonators [30, 31], and logic gates [32, 33]. The SC allows a narrow beam

to propagate in the PC without engineered defects or physical channel and hence it may simplify fabrication of some PC-based devices. The SC-specified PCs are insensitive to the incident position so that light can be self-collimated by the structure irrespective of the position at which the beams are incident. Then alignment of beams in the SC-based PCs is relatively straightforward.

Not only the SC-based PCs are incident-position invariant. There is also a possibility to obtain flat equal-frequency contours (EFCs), in which the SC is insensitive even to the angle of incidence. The EFC often referred to as iso-frequency or wave vector diagram is essential for the SC studies. Indeed, the band diagram which is a 'map' of the available $\omega(k)$ states shows the states only around the boundaries of the Brillouin zone. Instead, a contour plot $\omega(k_x, k_y)$ in the (k_x, k_y) plane reveals (periodic) curves of constant ω in all of the points within the Brillouin zone. The EFCs for optically isotropic materials (e.g., air) are circles, with the radius of each EFC representing the wave number $(2\pi n/\lambda)$ of the corresponding incident light, where n is the refractive index of the material and λ the incident wavelength. In this case, light propagation follows the Snell's law. On the other hand, the EFCs for anisotropic materials (e.g., many PCs) can manifest different shapes. As a result, one can manipulate the beam propagation in such anisotropic materials by engineering the shape of their EFCs in order to create a variety of interesting and non-conventional optical properties promising for many applications.

In the past, researchers have mainly concentrated at single particular performances of the SC, e.g. at increasing the collimating efficiency [34], reducing reflection on the input PC surface [35, 36], broadening the working frequency range [2, 15, 37], expanding the incident-angle range [2, 11, 23, 37, 38] and implementation of polarization-insensitive SC [14, 22, 39–42], among many instances. The three latter aspects are extremely attractive from the viewpoint of applications in future photonic integrated systems. Really, it would be very useful if the SC could be realized in the same working frequency range for the both polarizations, thus supporting an all-angle and broad-band SC property in the same structure. In its turn, this would imply an all-angle, polarization-insensitive and broad-band SC. These three characteristics can greatly enhance the efficiency of the SC and extend its applications [14]. Notice that most of the works reported so far support only one special polarization for the all-angle and broad-band SC, or the all-angle polarization insensitivity is limited to some frequency ranges only [2, 11, 14, 15, 22, 23, 37–44]. To the best of our knowledge, there have been no reports on the all-angle, polarization-insensitive and, at the same time, relatively broad-band SC.

The present article is therefore focused on the studies of the all-angle, broad-band and polarization-insensitive SC in a 2D square-lattice PC. In particular, we report on the choice of parameters for the 2D square-array PC structure based on the results achieved with plane-wave expansion (PWE) and finite-difference time-domain (FDTD) methods.

The article is organized as follows. First, we explain the reasons why we choose 2D square-array PCs among many other structures for the purpose of all-angle, polarization-insensitive and broad-band SC, and analyze the conditions needed to satisfy the all-angle SC in 2D square lattices. Next, using the analysis based on the PWE method, we motivate the hole-type structures as a basis for achieving the polarization-insensitive SC and the reasons for small deviations from the 'ideal' SC. Finally, we prove the appropriate outcomes using the FDTD analysis and at draw the main conclusions.

2. Suitability of 2D square-array PCs for the all-angle, broad-band and polarization-insensitive SC

Issuing from the researches reported on the SC phenomena so far, it becomes obvious that a 2D square-array PC with cylindrical scatterers represents one of the best candidates for designing self-

collimating waveguides. This is due to its simple structure compatible with the lithography fabrication processes developed up to date and, moreover, because it reveals the SC property in both the first and second bands along the ΓM and ΓX directions [45]. Indeed, if the all-angle, broad-band, polarization-insensitive SC can be achieved in the first band for the case when the PC is surrounded by air, the band would lie completely 'under the light line', and so the structure would suppress the out-of-plane scatterings and the losses [42], because the modes are index-guided and decay exponentially into the region of air. Furthermore, a 2D square-array PC supports a broad range of the SC frequencies and shows more tendencies for the large-angle SC [46].

Although the previous results obtained for the 2D square-array PCs prove that the 2D square array is a good candidate to reveal a large-angle and broad-band SC, there has been no comprehensive study of whether all the needed properties of the all-angle, broad-band and polarization-insensitive SC can be attained in a basic 2D square array, or not. In fact, here we imply demonstrating a possibility to combine all of these characteristics achieved by tailoring the index contrast, selecting a proper structure type and the corresponding radius, and considering slight compromises imposed on the 'degree of SC'. In other words, we will focus on achieving the all-angle, broad-band and polarization insensitive SC in the 2D square-array PCs.

It is known that the direction of propagation of light in a PC is governed by its dispersion surfaces, being defined by the group velocity $v_{group} = \partial\omega(k)/\partial k$. For the wave vector k belonging to flat parts of the dispersion surfaces, an excited Bloch wave propagates without diffraction through the PC and so the SC occurs. The SC can occur only under certain conditions. First, the PC structure is to manifest partially (or totally) flat EFCs. Second, at least one of these flat EFCs must intersect their corresponding k-vector 'conservation lines' (i.e., the lines indicating surface-parallel k-vector conservation) at the same frequency. On the other hand, the all-angle SC means that light with arbitrary incident angles can be self-collimated in the PC. Then the all-angle SC is possible only when the air contour's diameter for a specific frequency is smaller than the flat part of the EFC for a given PC structure [11] (see Fig. 1).

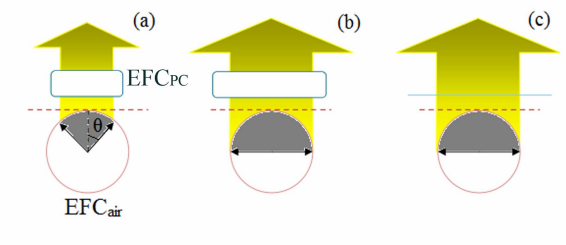

Fig. 1. Schematic example of EFCs for a PC (blue lines) and the corresponding air contours (circles) of the cases of (a) limited-angle SC; (b) all-angle SC using flat long EFCs and (c) all-angle SC using flat open EFCs. Black arrows indicate directions of the incident light and shaded areas angular ranges of collimation. Yellow arrows correspond to direction of the coupled-light group velocity in the PC structure for all of collimation-supporting incidence angles.

The SC efficiency can be significantly increased by expanding the incidence-angle range [2, 11, 23, 37, 38] or, finally, achieving the all-angle SC**.** According to the previous studies, the square lattice can ensure the large-angle SC [1], although no all-angle SC is strictly realizable in this structure for the case of flat open EFCs. Of course, a break in the geometrical symmetry of the square-lattice structure (changing the basic lattice to rectangular [23] or rhombic [11] ones, or changing the scatterer's shape [15, 47], etc.) can result in the all-angle SC based upon the flat open EFCs. However, here we wish to obtain the all-angle SC with no changes in the basic structure.

Then the only solution should be employing materials with a high refractive-index contrast. This idea has been recognized for the first time by Zhang et al. [38]. In particular, these authors have pointed out that an ultrahigh-index background material is a key issue in achieving the all-angle SC. They have also proved that the main parameter controlling the all-angle self-collimating behaviour of the 2D square-lattice PC is the the index of the background material rather than index contrast for the specific filling ratio.

3. Analysis of all-angle, broad-band and polarization-insensitive SC using the PWE and FDTD methods

To get the minimum index contrast satisfying the all-angle SC conditions, we study rod- and hole-type structures for the cases of different refractive indices separately. As important examples, below we illustrate the specific results derived for the refractive indices n = 3.4, 4.0, 4.5 and 6.0. In this work we have developed a software package called as an Rsoft Photonics CAD. In the present analysis, BandSOLVE and FullWAVE modules of this package are mainly utilized. A BandSOLVE is a simulation module for generating and analyzing photonic-band structures and EFCs, which is based on a known PWE technique for the periodic structures. We remind that the PWE is a widely spread numerical method for calculating band diagrams and EFCs of the PCs [48, 49]. This approach treats the Maxwell's equations as an eigenvalue problem, where the eigenvalues represent the angular frequencies of the existing modes in the PC and the eigenvectors are the amplitude coefficients of the fields. In the framework of the PWE method, the dielectric function and the field are expanded into Fourier series in the reciprocal k-space.

Note that, for different frequency ranges, the refractive indices mentioned above can be peculiar for different materials. Below we also assume that the medium where a light source is positioned is air while the working materials are lossless. Using the PWE method, we have studied the rod- and hole-type structures for different structural parameters and both TE and TM polarizations. The frequency has been represented in a normalized form as $a/\lambda = \omega a/2\pi c$, with a being the lattice constant. Different normalized frequencies have been considered, which correspond to the flat EFC for each PC with different index contrast and radius size r.

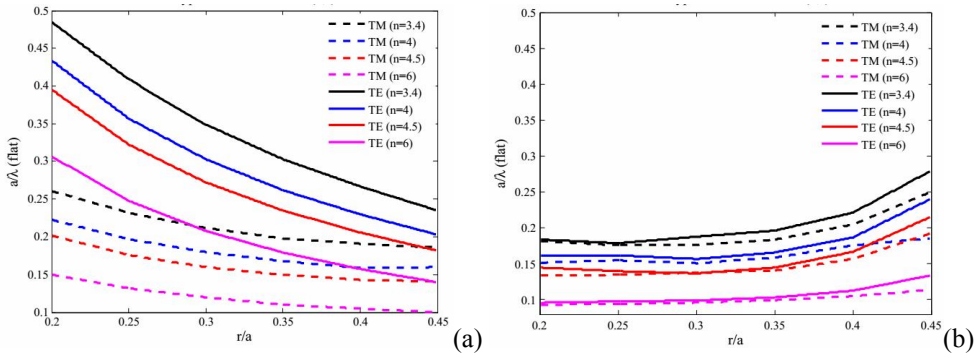

Fig. 2. Parameters a/λ_{flat} calculated for the 2D square-array PCs of the rod-type (a) and hole-type (b) for different structural parameters and light polarizations TE and TM. r denotes the radius of scatterers.

As illustrated in Fig. 2 for the both rod- and hole-type 2D square-array PCs, the normalized frequency corresponding to the flat EFC (a/λ_{flat}) decreases with increasing index contrast. As mentioned above, the PWE method has enabled us to survey possibilities for attaining the all-angle SC property and the corresponding bandwidths for the cases of rod- and hole-type 2D square-array PCs. A decrease in the a/λ_{flat} parameter eventually results in the all-angle, flat and long EFC so that

the all-angle SC can be achieved. According to our extensive calculations with the PWE method, the all-angle SC property occurs for the choices of parameters summarized in Table 1.

Table 1. Sets of parameters of the 2D square-array PC which support the all-angle SC.

n, r/a	Type of structure	Polarization
6.0, 0.20–0.45	rod	TM
6.0, 0.20–0.40	hole	TM
6.0, 0.25–0.40	hole	TE

Although either increase or decrease in the radiuses of the rods and the holes imposes decreasing a/λ_{flat} (see Fig. 2), the impact of the index contrast on the a/λ_{flat} shift towards lower normalized frequencies is stronger. In other terms, one can obtain the all-angle SC for different radiuses whenever the refractive index contrast becomes larger than a specific threshold value. Table 1 proves that achieving the all-angle SC with the 2D square arrays should rely on the index contrast rather than ultrahigh-index background. This consideration would result in easier choice of materials with more degrees of freedom.

Owing to this circumstance, in the present study we report the results for different refractive indices rather than different specific materials. Although a minimal index contrast should be introduced to gain the all-angle SC, we are free to choose a given material from fabrication technology considerations. Of course, the material should have the refractive index equal to or higher than the minimum index contrast in the frequency range where the all-angle SC is operated. Moreover, the minimum index-contrast requirement instead of that associated with the ultrahigh-index background material can result in achieving a polarization-insensitive SC property. Indeed, for the materials with a low refractive-index contrast for the scatterers and the background, the TE and TM bands should be close to each other in the band structure. As a result, a polarization-insensitive behaviour can be expected, according to the recent findings in the field of polarization-insensitive SC [44].

It is also evident from our results that the a/λ_{flat} differences between the TE and TM polarizations for the hole-type structures with the same structural parameters are smaller if compared with the rod-type structures. This fact implies that the hole-type structures are better candidates for achieving the all-angle and polarization-insensitive SC effect.

The only problem in achieving the all-angle, polarization-insensitive SC is that, for almost 'ideal' SCs with very small deviation angles ($\sim 1^{\text{o}}$) in the collimation direction, the relevant frequency ranges for the TE and TM polarizations do not overlap (see Table 2). The reason is that, for the 2D square-array PC, the EFCs are not perfectly flat and, therefore, only a partial SC is achievable. As a means to quantify the corresponding 'degree of SC', we take advantage of the maximum absolute refraction angle ($|\theta_p|_{\max}$). The angle $|\theta_p|_{\max}$ is the largest deviation of the propagation directions from the primary collimating direction. For the case of 'ideal' SC, we would have $|\theta_p|_{\max} = 0^{\text{o}}$. If different frequencies are simultaneously considered, the $|\theta_p|_{\max}$ parameter would imply the overall maximum referred to all of the frequencies chosen.

Of course, such a virtually collimated beam slightly diverges while propagating. However, when an ideal SC performance cannot be achievable for a broad-band 'all-angle' operation, slight compromises imposed on the degree of SC might be acceptable in order to improve the angular collimation range and the operating bandwidth. In this study, we describe the bandwidth as the ratio of the corresponding normalized frequency range where the phenomenon is supported to the

central frequency of that range, in a manner quite similar to the definition of the gap-to-midgap ratio employed in the discussions of photonic bandgap in PCs.

Using the PWE method, we have calculated the normalized frequency range for different structural parameters of the 2D hole-type square-array PCs and for a number of deviation angles ($|\theta_p|_{max}$=1, 2, 3, 4 and 5°). In this way we have selected an 'optimized structure' which reveals the maximum frequency range among all the others structures. It is the hole-type structure with $n = 6.0$ and $r = 0.3a$. The band structure has been derived for that optimized structure for the both TE/TM polarizations, as illustrated in Fig. 3a. Moreover, the EFC has been calculated for the optimized structure with $a/\lambda = 0.097$, which proves feasibility of the all-angle, polarization-insensitive SC for the above normalized frequency along the ΓM direction (see Fig. 3b).

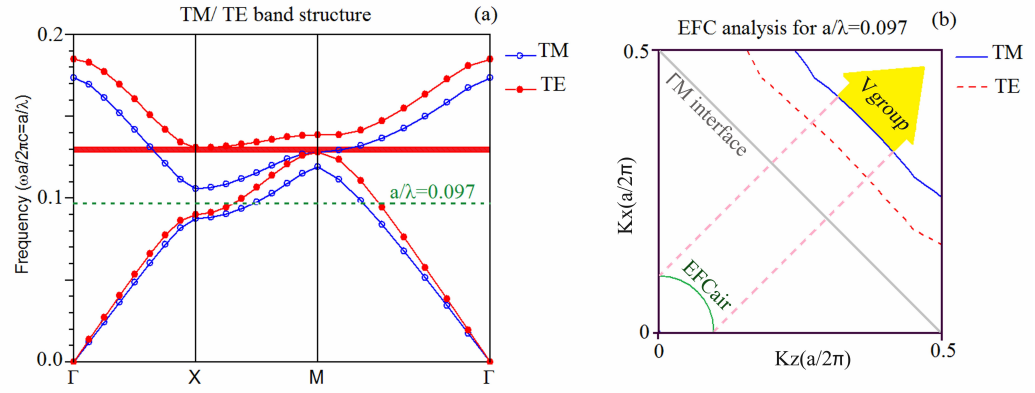

Fig. 3. (a) Band structure and (b) EFC calculated in the case of 'optimized structure' for the TE/TM polarizations at $a/\lambda = 0.097$ (see text).

From the results presented in Table 2 for the optimized structure it is evident that one has to accept a small deviation angle (at least 2°), which enables achieving simultaneously the all-angle and polarization-insensitive SC effect in the hole-type structure. Then the minimum index contrast satisfies the all-angle SC condition considered above. As seen from Table 2, the deviation angle as small as 2° allows one to obtain the all-angle, polarization-insensitive SC in the optimized structure with the bandwidth of 0.55%. In any practical applications, one can accept larger deviation angles, thus resulting in still broader bandwidths.

Table 2. Frequency ranges for the optimized structure (hole-type 2D square-array PC with $n = 6$, $r = 0.3a$) for different angles of deviation.

Deviation angle $\|\theta_p\|_{max}$, deg	Normalized frequency range for TE	Normalized frequency range for TM	Overlapping of normalized frequency ranges for TE and TM	$\Delta f/f_c$, %
1	0.09801–0.10045	0.095845–0.09678	–	–
2	0.09665–0.10157	0.095345–0.09719	0.09665–0.09719	0.55
3	0.0951–0.1027	0.09479–0.09762	0.0951–0.09762	2.61
4	0.0935–0.1036	0.0942–0.098	0.0942–0.098	3.95
5	0.0915–0.1045	0.0929–0.0983	0.0929–0.0983	5.64

Hence, by the above analyses we have demonstrated the SC effect which reveals simultaneously (i) all-angle, (ii) polarization-insensitive and (iii) broad-band features. To the best of our knowledge, this is the first study where these three attractive and urgently required properties are shown to be displayed by such a simple structure as a 2D square-array PC. Although we have had to accept a small deviation angle to combine all these properties at once, this departure from the 'ideal' case can cause no significant problems in small-sized, (e.g., integrated) devices. Also, the bandwidth can be broadened via increasing the acceptable deviation angle that depends on the application.

To further prove the applicability of our structure for the purpose of all-angle, polarization-insensitive SC, we have used the FullWAVE software module which employs the FDTD method. The latter method provides a rigorous solution to the Maxwell's equations. It represents a flexible technique for characterization of broad-band characteristics and visualization of fields [50]. The method allows for simulating almost any structures, including non-periodic and rather complicated ones. In addition, this scattering algorithm can also be employed to calculate the eigenmodes and obtain the band diagrams. In the frame of the FDTD method, the structures under study are represented by discrete grid points (a Yee's mesh [51]) in the spatial domain. Then we have computed the field components E and H at those grid points by iterating the time-dependent Maxwell's equations over time.

We have created the hole-type structure with the lattice size of $40a \times 40a$. A continuous Gaussian point source has been set in the centre of the structure. Its normalized frequency has been equal to $a/\lambda = 0.097$, which corresponds to the vicinity of the overlapped frequency range under the conditions appropriate for the all-angle, polarization-insensitive SC. A 'perfectly matched layer' has been used for the boundary conditions. It acts as a high-loss material and absorbs all the incident energy without producing reflections at the edges of the simulation region. This enables the field energy incident at the boundary to effectively leave the domain and so suits the best our simulation topology, when considering finite scales of our structure. The grid sizes are $\Delta x = \Delta z = a/32$ for both the transverse and propagation directions.

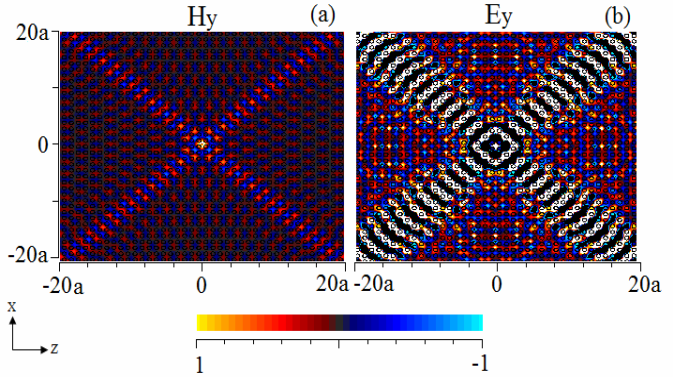

Fig. 4. Spatial distributions of the field components H_y (a) and E_y (b) calculated respectively for the TM and TE polarizations ($a/\lambda = 0.097$).

The results illustrated in Fig. 4 show that the light is collimated along the ΓM directions in the structure for the both polarizations. This proves that the structure supports the all-angle and polarization-insensitive SC characteristics along this specific direction. Such a situation is also expected from the results obtained using the PWE analysis.

4. Conclusion

Summing up, we have investigated the possibilities for achieving the broad-band, all-angle and polarization-insensitive SC effect in the 2D square-array PCs. In order to obtain the all-angle SC property, a threshold index contrast should be exceeded, above which the all-angle, flat and long EFC results. To ensure the polarization insensitivity, we have chosen the hole-type structure that reveals less polarization dependence when compared with the rod-type structure. Furthermore, a small deviation from the 'ideal' SC conditions has been suggested to achieve all-angle, polarization-insensitive and broad-band characteristics simultaneously in the same structure. Our calculation results achieved with the PWE method have been proven further using the more general FDTD method.

References

1. Chigrin D N, Torres S and Tayeb G, 2003. Self-guiding in two-dimensional photonic crystals. Opt. Express. **11**: 1203–1211.
2. Hamam R E, Johnson S G, Joannopoulos J D and Soljacic M, 2009. Broadband super-collimation in a hybrid photonic crystal structure. Opt. Express. **17**: 8109–8118.
3. Shuai F and Yi-Quan W, 2011. Light propagation properties of two-dimensional photonic crystal channel filters with elliptical micro-cavities. Chinese Phys. B. **20**: 104207.
4. Prather D W, Sharkawy A, McBride S, Zanzucchi P, Chen C, Pustai D, Venkataraman S, Murakowski J and Schneider G, 2003. Dispersion engineering of photonic crystals. Proc. SPIE. **5184**: 30–40.
5. Jovanovic D, Gajic R, and Hingerl K, 2008. Refraction and band isotropy in 2D square-like Archimedean photonic crystal lattices. Opt. Express. **16**: 4048-4058.
6. Notomi M, 2000. Theory of light propagation in strongly modulated photonic crystals: Refraction like behavior in the vicinity of the photonic band gap. Phys. Rev. B. **62**: 10696–10705.
7. Gajic R, Kuchar F and K. Hingerl, 2006. All-angle left-handed negative refraction in Kagome and honeycomb lattice photonic crystals. Phys. Rev. B. **73**: 165310-17.
8. Gaji c R, Kuchar F, Jovanovic D and Hingerl K, 2007. Negative refraction and left-handedness in 2D Archimedean lattice photonic crystals. Mater. Sci. Forum. **555**: 83–88.
9. Wu L J, Karle T and Krauss T F, 2002. Super-prism phenomena in planar photonic crystals. IEEE J. Quant. Electron. **38**: 915–918.
10. Akosman A E, Kurt H and Ozbay E, 2011. Compact wavelength de-multiplexer design using slow light regime of photonic crystal waveguides. Opt. Express. **19**: 24129–24138.
11. Wu Z H, Yang H J, Jiang P and He X J, 2012. All-angle self-collimation in two-dimensional rhombic-lattice photonic crystals. J. Opt. **14**: 015002.
12. Shih T M, Dahelm M, Petrich G, Soljacic M, Ippen E, Kolodziejski L, Hall K and Kesler M, 2008. Supercollimation in photonic crystals composed of silicon rods. Appl. Phys. Lett. **93**: 131111.
13. Shuai C F, Zhong W and Quan W Y, 2012. Controlling the self-collimation characteristics of a near-infrared two-dimensional metallic photonic crystal. Chin. Phys. B. **21**: 114212.
14. Jiang W L and Li X, 2013. Polarization-insensitive and broad-angle self-collimation in a two-dimensional photonic crystal with rectangular air holes. Appl. Opt. **52**: 6676–6684.
15. Liang W Y, Yin C P, Dong J W, Leng F C and Wang H Z, 2010. Super-broadband non-diffraction guiding modes in photonic crystals with elliptical rods. J. Phys. D: Appl. Phys. **43**: 075103.

16. Kim M W, Kim T T, Kim J E, Park H Y and Kee C S, 2007. Experimental demonstration of bending and splitting of self-collimated beams in two-dimensional photonic crystals. Appl. Phys. Lett, **90**: 1131211-3.
17. Wu L J and Krauss T F, 2003. Beam steering in planar-photonic crystals: from superprism to supercollimator. J. Lightwave Technol. **21**: 561–566.
18. Kosaka H, Tomita A, Notomi M, Tamamura T, Sato T and Kawakami S, 1999. Self-collimating phenomena in photonic crystals. Appl. Phys. Lett. **74**: 1212–1214.
19. Xu X Q and Yang H, 2010. Optimize design super collimation in square lattice two-dimensional photonic crystals. Optik – Int. J. Light Elect. Opt. **121**: 1573–1576.
20. Gao D, Zhou Z and Citrin D S, 2008. Self-collimated waveguide bends and partial bandgap reflection of photonic crystals with parallelogram lattice. J. Opt. Soc. Amer. A. **25**: 791–795.
21. Prather D W, Shi S, Miao B, Pustai D M, Venkataraman S, Sharkawy A S, Schneider G J and Murakowski J A, 2004. Ultralow-loss photonic crystal waveguides based on the self-collimation effect. Photonic Crystal Materials and Devices II, SPIE. **5360**: 175.
22. Hou G. J, Wu H M and Zhou Z P, 2009. Polarization insensitive self-collimation waveguide in square lattice annular photonic crystals. Opt. Commun. **282**: 3172–3176.
23. Xu C Y, Lan S, Guo Q, Hu W and Wu L J, 2008. The all-angle self-collimating phenomenon in photonic crystals with rectangular symmetry. J. Opt. A. **10**: 085201.
24. Matthews A F, 2009. Experimental demonstration of self-collimation beaming and splitting in photonic crystals at microwave frequencies. Opt. Commun. **282**: 1789–1792.
25. Zhang Z Y and Li B, 2007. Optical switches and logic gates based on self-collimated beams in two-dimensional photonic crystals. Opt. Express. **15**: 9287–9292.
26. Zheng W G, Zhao D, Zhang W and Liu Y, 2014. Wavelength-division multiplexing system with photonic crystal self-collimation and co- directional coupling effect. Optik – Int.J. Light Elect. Opt., **125**: 2638– 2641.
27. Wang W Y, Xue Q and Zheng W, 2012. Photonic crystal self-collimation sensor. Opt. Express. **20**: 12111–12118.
28. Chen X Y, Qiu Y S, Wang Y F and Ni B, 2008. Tunable photonic crystal Mach-Zehnder interferometer based on self-collimation effect. Chinese Phys. Lett. **25**: 4307–4310.
29. Zhang W, Liu J, Huang W P and Zhao W, 2009. Self-collimating photonic-crystal wave plates. Opt. Lett. **34**: 2676–2678.
30. Iliew R, Etrich C, Pertsch T, Lederer F and Staliunas K, 2008. Subdiffractive all-photonic crystal Fabry-Perot resonators. Opt. Lett. **33**: 2695–2697.
31. Xiao-Peng S, Kui H, Fang Y, Peng L H, Yu Z Z and Qi Z, 2008. New configuration of ring resonator in photonic crystal based on self-collimation. Chinese Phys. Lett. **25**: 4288.
32. Christina X S, 2012. Design of optical logic gates using self-collimated beams in 2D photonic crystal. Photon. Sens. **2**: 173–179.
33. Lin W P and Kuo H L, 2012. Design of optical nor logic gates using two dimension photonic crystals. Amer. J. Mod. Phys. **2**: 144–147.
34. Rumpf R C, 2013. Optimization of planar self-collimating photonic crystals. J. Opt. Soc. Amer. A. **30**: 1297–1304.
35. Lawrence F J, Dossou K B and de Sterke C M, 2008. Antireflection coatings for two-dimensional photonic crystals using a rigorous impedance definition. Appl. Phys. Lett. **93**: 131111.
36. Park J M, Park H R and Lee M H, 2010. Self-collimating photonic crystal antireflection structure for both TE and TM polarizations. Opt. Express. **18**: 13083–13093.
37. Chuang Y C, 2010. Complex rhombus lattice photonic crystals for broadband all-angle self-collimation J. Opt. **12**: 035102.

38. Zhang C H, Chen L, Zhu H, Qian L and Fan D, 2010. Full-angle collimations of two-dimensional photonic crystals with ultrahigh-index background materials. J. Opt. **12**: 045103–045108.
39. Xu C Y, Lan S, Dai Q F, Guo Q and Wu L J, 2009. Polarization-independent self-collimation based on pill-void photonic crystals with square symmetry. Opt. Express. **17**: 4903-12.
40. Shen X P, Shen Y F, Li H P, Xiao Z W and Zheng J, 2006. Self-collimation of unpolarized electromagnetic waves in 2D photonic crystals. Acta Phys. Sin. **55**: 2760–2764.
41. Cicek U A, 2009. Polarization-independent waveguiding with annular photonic crystal. Opt. Express. **17**:18381–18386.
42. Zabelin D V, Thomas N L, Houdr'e R, Kotlyar M V, O'Faolin L and Krauss T F, 2007. Self-collimating photonic crystal polarization beam splitter. Opt. Lett. **32**: 530–532.
43. Turduev G M and Kurt H, 2012. Modified annular photonic crystals with enhanced dispersion relations: polarization insensitive self-collimation and nanophotonic wire waveguide designs. J. Opt. Soc. Amer. B. **29**: 1589–1598.
44. Jiang L Y and Li X Y, 2014. Study on the polarization-insensitive self-collimation behavior in two-dimensional all-solid photonic crystals. J. Opt. **43**: 108–116.
45. Witzens L J and Scherer A, 2002. Self-collimation in planar photonic crystals. IEEE J. Selected Topics In Quantum Electron. **8**: 1246–1257.
46. Ogawa O Y and Iida Y, 2005. Study on self-collimated light-focusing device using the 2-D photonic crystal with a parallelogram lattice. J. Lightwave Technol. **23**: 4374.
47. Jiang W L and Li X, 2013. Polarization-insensitive and broad-angle self-collimation in a two-dimensional photonic crystal with rectangular air holes. Appl. Opt. **52**: 6676–6684.
48. Guo S and Albin S, 2003. Simple plane wave implementation for photonic crystal calculations. Opt. Express. **11**: 167–175.
49. Rumpf R C, 2013. Optimization of planar self-collimating photonic crystals. J. Opt. Soc. Amer. A. **30**: 1297–1304.
50. Taflove A, and Hagness S C, Computational electrodynamics: the finite difference time domain method (Artech House, Inc., 2000).
51. Yee K S, 1966. Numerical solution of initial boundary value problems involving Maxwell's equations in isotropic media. IEEE Trans. Antennas and Propagation. **14**: 302.

Noori M., Soroosh M. and Baghban H. 2015. An approach to achieve all-angle, polarization-insensitive and broad-band self-collimation in 2D square-lattice photonic crystals. Ukr.J.Phys.Opt. **16**: 85 – 94.

Анотація. *Ми вивчили можливість одночасного отримання повнокутового, поляризаційно нечутливого і широкосмугового самоколімування (СК) на єдиній структурі. Це відповідає одній із актуальних вимог в галузі оптичного інтегрування. Для досягнення цих привабливих рис СК на двовимірних фотонних кристалах із квадратною матрицею було використано низку підходів і розрахункові перевірки на основі методів розкладу за плоскими хвилями і скінченних різниць часових інтервалів. Ми не ускладнювали базову структуру для досягнення СК і зберегли її просту геометрію. СК з'являється для оптичного матеріалу в структурі діркового типу з високим показником заломлення . Наші результати засвідчили, що СК у структурі діркового типу слабше залежить від поляризації світла, ніж у схожій структурі стрижневого типу. Наша оптимізована структура для СК має ширину смуги* $\Delta f/f_c = 2{,}61\%$ *і підтримує повнокутове СК для обох поляризації TE і TM коштом незначного (~* 3^o*) відхилення світла від єдиного напрямку колімування. Останній недолік не є суттєвим для інтегрованих оптичних пристроїв.*